PERGAMON

International Journal of Solids and Structures 40 (2003) 1547–1565

INTERNATIONAL JOURNAL OF SOLIDS and STRUCTURES

www.elsevier.com/locate/ijsolstr

On a bounded elliptic elastic inclusion in plane magnetoelasticity

Chun-Bo Lin

Department of Automation Engineering, Nan Kai College, Nantou 542, Taiwan, ROC

Received 6 February 2002; received in revised form 8 November 2002

Abstract

The problem of an elliptic inclusion embedded in an infinite matrix subjected to a uniform magnetic induction is considered in this paper. Basing upon the two-dimensional magnetoelastic formulation, the technique of conformal mapping, and the method of analytical continuation, a general solution of magnetic field quantities and the magnetoelastic stresses are obtained for both the matrix and the inclusion. Comparison is made with several special cases of which the analytical solutions can be found in the literature, which shows that the solutions presented here are general and exact. Moreover, the magnetoelastic stresses at the interface between the inclusion and the matrix are presented with figures.

Keywords: Elliptical inclusion; Analytical continuation

1. Introduction

It is known that there are some defects in the form of cracks, voids, inclusions, etc., existing in most engineering materials. In view of its flexibility to cover a wide variety of particular cases, such as line or circular inclusions, the elliptic inhomogeneity problems have received considerable interest. Early work by Hardiman (1954) and Eshelby (1957) showed that a constant stress state within the elliptic inclusion is induced by a uniform stress applied at infinity. By the use of conformal mapping and the Laurent series expansion of complex functions, Gong and Meguid (1992) investigated the elliptical inclusion problem under the action of antiplane shear.

For the defects in a ferromagnetic solid subjected to magnetic loading, many earlier investigators have devoted to the crack problems. Based upon the linear theory of Pao and Yeh (1973) and the technique of integral transformation, Shindo (1977) and Shindo et al. (1999) derived the magnetoelastic fields for the soft ferromagnetic material containing a line crack. Lin and Yeh (2002) solved the crack problem in plane magnetoelasticity by the use of complex variable method. The J-integrals around the cracks within soft ferromagnets (Sabir and Maugin, 1996) and hard ferromagnets (Fomethe and Maugin, 1998) were

E-mail address: cblin@nkc.edu.tw (C.-B. Lin).

doi:10.1016/S0020-7683(02)00667-4

derived on the basis of the rotationally invariant quasi-magnetostatic theory. On the magnetoelastic problem with curvilinear boundary, van de Ven (1984) used Mathieu functions to study the magnetic buckling of a beam of elliptic cross-section under transverse magnetic induction. Although the elastic inclusion problems (summarized by Mura, 1988) and the crack problems in plane magnetoelasticity were investigated extensively, the corresponding magnetoelastic problem of elliptic inclusion is still an interesting and new study of research due to the widespread use of the application of magnetoelasticity in various fields.

The objective of this paper is to find the magnetoelastic fields induced by the applied magnetic fields on an infinite matrix containing an elliptic elastic inclusion. Since the formulation of complex variable method in elasticity (Muskhelishvili, 1953; England, 1971) and magnetoelasticity (Lin and Yeh, 2002) is compact, it is adopted in the following work. We introduce the complex potential functions of magnetic and magnetoelastic fields which satisfy the corresponding governing equations. By the method of analytical continuation together with the proper boundary conditions, the magnetic and the magnetoelastic functions can be solved explicitly. It is worthy to mention that we introduce a pertinent function to convert the boundary condition into a form without the complex conjugate of the space variables. The present solution which satisfies both the governing equations and the boundary conditions simultaneously is exact. Due to that the general solutions have not been found in the literature, the results of several special cases, such as elliptic hole, elliptic rigid inclusion and air matrix, etc., are also provided and compared with the existing analytical solutions. Hence the exactness of the present solutions can be guaranteed.

2. Formulations of magnetic fields

A soft ferromagnetic medium containing an elliptical inhomogeneity under a remote uniform magnetic induction is considered in the present study (see Fig. 1). The regions which are occupied by the matrix and the inclusion are denoted by S_1 and S_2 respectively. Basing on the two-dimensional theory of magnetoelasticity, the magnetic fields can be expressed as (Lin and Yeh, 2002)

$$B_x + \mathrm{i}B_y = \mu_0\mu_r(H_x + \mathrm{i}H_y) = \mu_0\mu_r\overline{h'(z)} \tag{1}$$

where

$$h(z) = \varphi(x,y) + \mathrm{i}\gamma(x,y) \tag{2}$$

is a magnetic potential function of the complex variable $z\ (= x + \mathrm{i}y)$, prime indicates differentiation with respect to z and overhead bar denotes complex conjugate. The symbols B_j and H_k are magnetic induction (or magnetic flux density) and magnetic intensity, $\mu_0 = 4\pi \times 10^{-7}\ \mathrm{N/A^2}$ is a universal constant and μ_r is the relative magnetic permeability.

Let us introduce the transformation function

$$z = \frac{a+b}{2}\zeta + \frac{a-b}{2}\zeta^{-1} \tag{3}$$

which will map the region outside the elliptic inclusion in z-plane onto the exterior of the circle $|\zeta| = 1$ in the transformed ζ-plane and the region inside the elliptic inclusion onto the interior of annular region between the unit circle and a circle of radius $\sqrt{\rho}$. Here ρ is related to the major semi-axis a and minor semi-axis b of the elliptic inclusion in z-plane by

$$\rho = \frac{a-b}{a+b} \tag{4}$$

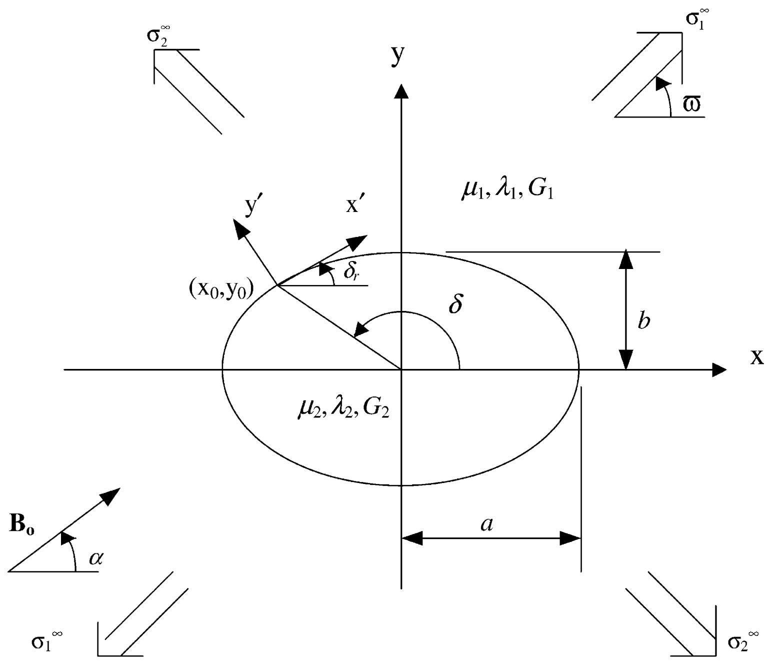

Fig. 1. The far field stresses and magnetic induction on a matrix with an elliptic inclusion.

It is observed that the radius $\sqrt{\rho}$ is less than 1. The transformation in Eq. (3) is single valued in the exterior region of inclusion but it becomes double valued within the elliptic inclusion. To remedy the discontinuity, the following restriction should be satisfied for the relevant functions (Gong and Meguid, 1992)

$$p(\sqrt{\rho}\sigma) = p(\sqrt{\rho}/\sigma) \tag{5}$$

where $\sigma = e^{i\theta}$.

In this study, a remote uniform magnetic induction is applied on a soft ferromagnetic body with an elliptic inclusion. Using Eq. (4) and the technique of conformal mapping, the complex potential function $h_1(\zeta)$ in S_1 can be written as

$$h_1(\zeta) = h^*(\zeta) + h_0(\zeta) \quad \text{for } \zeta \in S_1 \tag{6}$$

where

$$h_0(\zeta) = gz = g\left(\frac{a+b}{2}\zeta + \frac{a-b}{2}\zeta^{-1}\right) \tag{7}$$

with

$$g = \frac{B_0 e^{-i\alpha}}{\mu_0 \mu_{r1}} \tag{8}$$

indicates the magnetic field of a remote uniform magnetic induction $B_0 e^{-i\alpha}(= B_{0x} - iB_{0y})$ which is directed at an angle α with respect to the x-axis. Notice that $h_1(\zeta)$ corresponds to the magnetic function $h_1(z)$ in the transformed ζ-plane.

Since the magnetic function $h_2(\zeta)$ is holomorphic in the annular area S_2 of the mapped ζ-plane, it can be represented by a Taylor's expansion as

$$h_2(\zeta) = \sum_{k=-\infty}^{\infty} e_k \zeta^k \quad \text{for } \zeta \in S_2 \tag{9}$$

In view of Eq. (9), we may neglect the term e_0 which has no contribution on the magnetic field. Applying Eq. (5), the coefficient e_k in Eq. (9) satisfies

$$e_{-k} = \rho^k e_k \tag{10}$$

where ρ is defined in Eq. (4). In the present work, the inclusion and the matrix are assumed to be perfectly bonded along their interface, the boundary conditions of magnetic fields can be expressed mathematically as (Lin and Yeh, 2002)

$$\varphi_1 = \varphi_2, \quad \mu_0\mu_{r1}\gamma_1 = \mu_0\mu_{r2}\gamma_2 \quad \text{along the interface } \zeta = \sigma = e^{i\theta} \tag{11}$$

where

$$\varphi_j = [h_j(\zeta) + \overline{h_j(\zeta)}]/2, \quad \gamma_j = [h_j(\zeta) - \overline{h_j(\zeta)}]/(2i) \tag{12}$$

can be obtained from Eq. (2). Employing Eqs. (6)–(10) and (12), the continuity conditions of magnetic fields in Eq. (11) lead to

$$\begin{aligned} &h^*(\sigma) + (\bar{g} + g\rho)\frac{a+b}{2}\sigma^{-1} - \sum_{k=1}^{\infty} \bar{e}_k \sigma^{-k} - \sum_{k=1}^{\infty} \rho^k e_k \sigma^{-k} \\ &\quad = -\bar{h}^*\left(\frac{1}{\sigma}\right) - (g + \bar{g}\rho)\frac{a+b}{2}\sigma + \sum_{k=1}^{\infty} e_k \sigma^k + \sum_{k=1}^{\infty} \bar{\rho}^k \bar{e}_k \sigma^k \end{aligned} \tag{13}$$

$$\begin{aligned} &\mu_0\mu_{r1}\left[h^*(\sigma) - (\bar{g} - g\rho)\frac{a+b}{2}\sigma^{-1}\right] + \mu_0\mu_{r2}\left(\sum_{k=1}^{\infty} \bar{e}_k \sigma^{-k} - \sum_{k=1}^{\infty} \rho^k e_k \sigma^{-k}\right) \\ &\quad = \mu_0\mu_{r1}\left[\bar{h}^*\left(\frac{1}{\sigma}\right) - (g - \bar{g}\rho)\frac{a+b}{2}\sigma\right] + \mu_0\mu_{r2}\left(\sum_{k=1}^{\infty} e_k \sigma^k - \sum_{k=1}^{\infty} \bar{\rho}^k \bar{e}_k \sigma^k\right) \end{aligned} \tag{14}$$

Basing on the properties of holomorphic functions and applying the method of analytical continuation, it is convenient to introduce a new set of complex functions $\eta_i(z)$ which are holomorphic in the entire domain as

$$\begin{aligned} \begin{bmatrix} \eta_1(\zeta) \\ \eta_2(\zeta) \end{bmatrix} &= \begin{bmatrix} 1 & -1 \\ \mu_0\mu_{r1} & \mu_0\mu_{r2} \end{bmatrix} \begin{bmatrix} h^*(\zeta) \\ \sum_{k=1}^{\infty} \bar{e}_k \zeta^{-k} \end{bmatrix} - \begin{bmatrix} 1 \\ \mu_0\mu_{r2} \end{bmatrix} \sum_{k=1}^{\infty} \rho^k e_k \zeta^{-k} \\ &\quad + \begin{bmatrix} 1 & 1 \\ -\mu_0\mu_{r1} & \mu_0\mu_{r1} \end{bmatrix} \begin{bmatrix} \bar{g} \\ g\rho \end{bmatrix} \frac{a+b}{2}\zeta^{-1} \quad \text{for } |\zeta| > 1 \end{aligned} \tag{15}$$

and

$$\begin{aligned} \begin{bmatrix} \eta_1(\zeta) \\ \eta_2(\zeta) \end{bmatrix} &= \begin{bmatrix} 1 & -1 \\ \mu_0\mu_{r2} & \mu_0\mu_{r1} \end{bmatrix} \begin{bmatrix} \sum_{k=1}^{\infty} e_k \zeta^k \\ \bar{h}^*\left(\frac{1}{\zeta}\right) \end{bmatrix} + \begin{bmatrix} 1 \\ -\mu_0\mu_{r2} \end{bmatrix} \sum_{k=1}^{\infty} \bar{\rho}^k \bar{e}_k \zeta^k \\ &\quad - \begin{bmatrix} 1 & 1 \\ \mu_0\mu_{r1} & -\mu_0\mu_{r1} \end{bmatrix} \begin{bmatrix} g \\ \bar{g}\rho \end{bmatrix} \frac{a+b}{2}\zeta \quad \text{for } |\zeta| < 1 \end{aligned} \tag{16}$$

On the basis of Liouville's theorem, the complex functions $\eta_1(\zeta)$ and $\eta_2(\zeta)$ that are holomorphic in the entire plane including the points at infinity are constant functions. Without loss of generality, we take $\eta_j(\zeta) = 0$ $(j = 1, 2)$. Thus, the following solution can be obtained from Eqs. (15) and (16) as

$$h^*(\zeta) = \left(\frac{\mu_{r1} - \mu_{r2}}{\mu_{r1} + \mu_{r2}}\bar{g} - g\rho\right)\frac{a+b}{2}\zeta^{-1} + \frac{2\mu_{r2}}{\mu_{r1} + \mu_{r2}}\sum_{k=1}^{\infty}\rho^k e_k \zeta^{-k} \tag{17}$$

$$\sum_{k=1}^{\infty} e_k \zeta^k = \frac{\mu_{r1}}{\mu_{r1} + \mu_{r2}} g(a+b)\zeta + \frac{\mu_{r2} - \mu_{r1}}{\mu_{r1} + \mu_{r2}}\sum_{k=1}^{\infty}\bar{\rho}^k \bar{e}_k \zeta^k \tag{18}$$

The coefficients e_k can be found by comparing the coefficients of ζ^k in Eq. (18). This gives

$$e_1 = \frac{\mu_{r1}\left[(\mu_{r2} + \mu_{r1})g(a+b) + (\mu_{r2} - \mu_{r1})\bar{g}(a-b)\right]}{(\mu_{r2} + \mu_{r1})^2 - (\mu_{r2} - \mu_{r1})^2\rho^2}, \qquad e_k = 0 \quad \text{for } k \neq 1, -1 \tag{19}$$

Inserting Eqs. (17) and (19) into (6) and (9) yields the complex potential $h_j(\zeta)$ in S_j $(j = 1, 2)$ as

$$h_1(\zeta) = \frac{a+b}{2} g\zeta + \beta\zeta^{-1} \tag{20}$$

$$h_2(\zeta) = e_1\zeta + \rho e_1 \zeta^{-1} \tag{21}$$

where

$$\beta = \frac{\mu_{r1} - \mu_{r2}}{\mu_{r1} + \mu_{r2}}\frac{a+b}{2}\bar{g} + \frac{2\mu_{r2}}{\mu_{r1} + \mu_{r2}}\rho e_1 \tag{22}$$

For the special case of the homogeneous magnetic problem (i.e. $\mu_{r1} = \mu_{r2}$), it is easy to verify that

$$h_1(\zeta) = h_2(\zeta) = gz \tag{23}$$

Applying Eq. (3), we have

$$\zeta = \frac{z + \sqrt{z^2 - (a^2 - b^2)}}{a+b}, \quad \zeta^{-1} = \frac{z - \sqrt{z^2 - (a^2 - b^2)}}{a-b} \tag{24}$$

Here the sign convention in Eq. (24) is chosen to assure the mapping between the points of $|z| \gg 1$ and $|\zeta| \gg 1$.

In order to express the magnetic potential function in z-plane, we introduce the following transformation

$$h_j'(z) = h_j'(\zeta)\frac{d\zeta}{dz} = \frac{h_j'(\zeta)}{m'(\zeta)}, \quad j = 1, 2 \tag{25}$$

Thus, the magnetic fields in both the matrix and the inclusion can be expressed in terms of z via the use of Eqs. (1), (20), (21), (24) and (25). It follows

$$(H_x + iH_y)_1 = \frac{1}{\mu_0\mu_{r1}}(B_x + iB_y)_1 = \overline{h_1'(z)} = \left(\frac{\bar{g}}{2} + \frac{\bar{\beta}}{a-b}\right) + \left(\frac{\bar{g}}{2} - \frac{\bar{\beta}}{a-b}\right)\frac{\bar{z}}{\sqrt{\bar{z}^2 - (a^2 - b^2)}} \tag{26}$$

$$(H_x + iH_y)_2 = \frac{1}{\mu_0\mu_{r2}}(B_x + iB_y)_2 = \overline{h_2'(z)} = \frac{2\bar{e}_1}{a+b} \tag{27}$$

which reveals that the magnetic fields in S_2 is uniform.

3. Magnetoelastic stresses induced by circular inclusion

Basing on the complex formulation of the plane magnetoelasticity (Lin and Yeh, 2002), the resultant force acting on the material to the left of the arbitrary arc AB can be written as

$$f_x^{(j)} + \mathrm{i} f_y^{(j)} = -\mathrm{i}\left[\phi_j(z) + z\overline{\phi_j'(z)} + \overline{\psi_j(z)} + \mu_0\chi_j\int_A^B h_j'(z)\overline{h_j'(z)}\,\mathrm{d}z - \frac{\mu_0}{2}(\mu_{\mathrm{r}j} + \chi_j)\int_A^B \overline{h_j'(z)}\,\overline{h_j'(z)}\,\mathrm{d}\bar{z}\right] \quad j = 1,2 \tag{28}$$

where the quantities with superscript or subscript j will be referred to S_j $(j = 1,2)$, i.e. the magnetic susceptibility χ_j $(= \mu_{\mathrm{r}j} - 1)$ and the complex potential functions $\phi_j(z)$ and $\psi_j(z)$ of stresses are defined in the corresponding region S_j. The displacements can be represented as

$$u_x^{(j)} + \mathrm{i} u_y^{(j)} = \frac{1}{2G_j}\left[\kappa_j\phi_j(z) - z\overline{\phi_j'(z)} - \overline{\psi_j(z)} - \frac{G_j}{(\lambda_j + 2G_j)}\mu_0\chi_j h_j(z)\overline{h_j'(z)}\right] \quad j = 1,2 \tag{29}$$

where the symbols λ_j and G_j are Laméys constants and $\kappa_j = (\lambda_j + 3G_j)/(\lambda_j + G_j) = 3\text{–}4\nu_j$ for plane strain (England, 1971). The symbol ν_j denotes the Poisson's ratio in S_j. It is remarked that those terms related to body force are omitted in Eqs. (28) and (29). The stress components take the form

$$\begin{aligned} \left(t_{xx}^{(j)} + t_{yy}^{(j)}\right)^{\mathrm{T}} &= \left(t_{xx}^{(j)} + t_{yy}^{(j)}\right) + \left(t_{xx}^{(j)} + t_{yy}^{(j)}\right)^{\mathrm{M}} \\ \left(t_{yy}^{(j)} - \mathrm{i}t_{xy}^{(j)}\right)^{\mathrm{T}} &= \left(t_{yy}^{(j)} - \mathrm{i}t_{xy}^{(j)}\right) + \left(t_{yy}^{(j)} - \mathrm{i}t_{xy}^{(j)}\right)^{\mathrm{M}} \end{aligned} \tag{30}$$

where

$$\begin{aligned} &\left(t_{xx}^{(j)} + t_{yy}^{(j)}\right) = 2\left[\phi_j'(z) + \overline{\phi_j'(z)}\right] + \mu_0\chi_j h_j'(z)\overline{h_j'(z)}, \quad \left(t_{xx}^{(j)} + t_{yy}^{(j)}\right)^{\mathrm{M}} = \mu_0\chi_j h_j'(z)\overline{h_j'(z)}, \\ &\left(t_{yy}^{(j)} - \mathrm{i}t_{xy}^{(j)}\right) = \phi_j'(z) + \overline{\phi_j'(z)} + \left[z\overline{\phi_j''(z)} + \overline{\psi_j'(z)}\right] + \frac{1}{2}\mu_0\chi_j\left[h_j'(z)\overline{h_j'(z)} - \overline{h_j'(z)}\,\overline{h_j'(z)}\right], \\ &\left(t_{yy}^{(j)} - \mathrm{i}t_{xy}^{(j)}\right)^{\mathrm{M}} = \frac{1}{2}\mu_0\left[\chi_j h_j'(z)\overline{h_j'(z)} - \mu_{\mathrm{r}j}\overline{h_j'(z)}\,\overline{h_j'(z)}\right] \end{aligned} \tag{31}$$

In Eq. (30), the stress components with superscript T indicate the total stresses which are the sum of the Maxwell stresses with superscript M and the magnetoelastic stresses. The Maxwell stresses which are not related to the deformation are defined artificially just for the sake of convenience. Namely, the magnetoelastic stresses rather than the total stresses are physically practical in spite of that the total stresses are continuous across the boundary (Pao and Yeh, 1973).

By proper rearrangement, Eqs. (28) and (29) lead to

$$\mathbf{f} = \mathrm{Re}[\mathbf{A}\boldsymbol{\Phi}(\zeta,\bar{\zeta}) + \mathbf{p}(\zeta,\bar{\zeta})], \quad \mathbf{f}^* = \mathrm{Re}[\mathbf{A}\boldsymbol{\Phi}^*(\zeta,\bar{\zeta}) + \mathbf{p}^*(\zeta,\bar{\zeta})] \tag{32}$$

$$\mathbf{u} = \mathrm{Re}[\mathbf{L}\boldsymbol{\Phi}(\zeta,\bar{\zeta}) + \mathbf{q}(\zeta,\bar{\zeta})], \quad \mathbf{u}^* = \mathrm{Re}[\mathbf{L}^*\boldsymbol{\Phi}(\zeta,\bar{\zeta}) + \mathbf{q}^*(\zeta,\bar{\zeta})] \tag{33}$$

where

$$\begin{aligned}
&\mathbf{f}=\begin{bmatrix} f_x^{(1)} \\ f_y^{(1)} \end{bmatrix}, \quad \mathbf{f}^*=\begin{bmatrix} f_x^{(2)} \\ f_y^{(2)} \end{bmatrix}, \quad \mathbf{u}=\begin{bmatrix} u_x^{(1)} \\ u_y^{(1)} \end{bmatrix}, \quad \mathbf{u}^*=\begin{bmatrix} u_x^{(2)} \\ u_y^{(2)} \end{bmatrix},\\
&\mathbf{A}=\begin{bmatrix} -\mathrm{i} & \mathrm{i} \\ -1 & -1 \end{bmatrix}, \quad \mathbf{L}=\frac{1}{2G_1}\begin{bmatrix} \kappa_1 & -1 \\ -\mathrm{i}\kappa_1 & -\mathrm{i} \end{bmatrix}, \quad \mathbf{L}^*=\frac{1}{2G_2}\begin{bmatrix} \kappa_2 & -1 \\ -\mathrm{i}\kappa_2 & -\mathrm{i} \end{bmatrix}\\
&\mathbf{\Phi}(\zeta,\bar{\zeta})=\begin{bmatrix} \phi_1(\zeta) \\ \varpi_1(\zeta,\bar{\zeta}) \end{bmatrix}, \quad \mathbf{\Phi}^*(\zeta,\bar{\zeta})=\begin{bmatrix} \phi_2(\zeta) \\ \varpi_2(\zeta,\bar{\zeta}) \end{bmatrix},\\
&\mathbf{p}(z,\bar{z})=\begin{bmatrix} -\mathrm{i}p \\ -p \end{bmatrix}, \quad \mathbf{p}^*(z,\bar{z})=\begin{bmatrix} -\mathrm{i}p^* \\ -p^* \end{bmatrix}, \quad \mathbf{q}(z,\bar{z})=\begin{bmatrix} q \\ -\mathrm{i}q \end{bmatrix}, \quad \mathbf{q}^*(z,\bar{z})=\begin{bmatrix} q^* \\ -\mathrm{i}q^* \end{bmatrix}
\end{aligned} \tag{34}$$

with

$$\begin{aligned}
&\varpi_j(\zeta,\bar{\zeta})=\bar{z}\phi_j'(z)+\psi_j(z)=\left(\frac{a+b}{2}\bar{\zeta}+\frac{a-b}{2\bar{\zeta}}\right)\frac{\phi_j'(\zeta)}{m'(\zeta)}+\psi_j(\zeta), \quad j=1,2\\
&p=\mu_0\chi_1\int_s h_1'(z)\overline{h_1'(z)}\,\mathrm{d}z-\frac{\mu_0}{2}(\mu_{\mathrm{r}1}+\chi_1)\int_s \overline{h_1'(z)}\,\overline{h_1'(z)}\,\mathrm{d}\bar{z}\\
&p^*=\mu_0\chi_2\int_s h_2'(z)\overline{h_2'(z)}\,\mathrm{d}z-\frac{\mu_0}{2}(\mu_{\mathrm{r}2}+\chi_2)\int_s \overline{h_2'(z)}\,\overline{h_2'(z)}\,\mathrm{d}\bar{z}\\
&q=-\frac{\mu_0\chi_1}{2(\lambda_1+2G_1)}h_1(z)\overline{h_1'(z)}, \quad q^*=-\frac{\mu_0\chi_2}{2(\lambda_2+2G_2)}h_2(z)\overline{h_2'(z)}
\end{aligned} \tag{35}$$

The surface tractions and the displacements should be continuous across the perfectly bonded interface between the inclusion and the matrix. i.e.

$$\mathbf{f}=\mathbf{f}^*, \quad \mathbf{u}=\mathbf{u}^* \quad \text{along the interface } \zeta=\sigma=\mathrm{e}^{\mathrm{i}\theta} \tag{36}$$

To solve the present problem, we introduce the function

$$\Psi(\zeta)=\begin{bmatrix} \phi_1(\zeta) \\ \upsilon_1(\zeta) \end{bmatrix}, \quad \Psi^*(\zeta)=\begin{bmatrix} \phi_2(\zeta) \\ \upsilon_2(\zeta) \end{bmatrix} \tag{37}$$

where

$$\upsilon_j(\zeta)=\left(\frac{a+b}{2\zeta}+\frac{a-b}{2}\zeta\right)\frac{\phi_j'(\zeta)}{m'(\zeta)}+\psi_j(\zeta), \quad j=1,2 \tag{38}$$

Applying Eq. (3) and using the relation $\bar{\sigma}=1/\sigma$ along the interface, it is easy to verify that

$$\varpi_j(\sigma,\bar{\sigma})=\upsilon_j(\sigma), \quad \mathbf{\Phi}(\sigma,\bar{\sigma})=\Psi(\sigma), \quad \mathbf{\Phi}^*(\sigma,\bar{\sigma})=\Psi^*(\sigma) \tag{39}$$

This means that the boundary conditions can now be converted into a form involving σ only. Thus, the problem becomes to determine the complex functions $\Psi(\zeta)$ and $\Psi^*(\zeta)$ which are expressed in terms of the space variable ζ rather than to solve the complex functions $\mathbf{\Phi}(\zeta,\bar{\zeta})$ and $\mathbf{\Phi}^*(\zeta,\bar{\zeta})$ which are related to both ζ and $\bar{\zeta}$. In order to satisfy the holomorphic requirement on S_1 and S_2, the functions $\Psi(\zeta)$ and $\Psi^*(\zeta)$ must take the form

$$\Psi(\zeta)=\mathbf{r}(\zeta)+\mathbf{s}\zeta, \quad \Psi^*(\zeta)=\sum_{k=-\infty}^{\infty}\boldsymbol{\omega}_k\zeta^k \tag{40}$$

where

$$\boldsymbol{\omega}_{-k} = \rho^k \boldsymbol{\omega}_k \tag{41}$$

The vector **s** in Eq. (40) can be solved from the limiting values of stress functions $\phi_1'(\zeta)$ and $\psi_1'(\zeta)$ at infinity as

$$\phi_1'(\zeta) = \frac{a+b}{2}\left[\Gamma + \frac{1}{2\mu_0}\left(\frac{1}{4} - \frac{\chi_1}{\mu_{r1}^2}\right)(B_{0x}^2 + B_{0y}^2)\right] + \mathrm{O}\left(\frac{1}{\zeta}\right) \quad \text{for } |\zeta| \gg 1 \tag{42}$$

$$\psi_1'(\zeta) = \frac{a+b}{2}\left[\Gamma' - \frac{1}{2\mu_0}\left(\frac{1}{2} - \frac{\mu_{r1}+\chi_1}{\mu_{r1}^2}\right)(B_{0x}^2 - 2\mathrm{i}B_{0x}B_{0y} - B_{0y}^2)\right] + \mathrm{O}\left(\frac{1}{\zeta}\right) \quad \text{for } |\zeta| \gg 1 \tag{43}$$

where

$$\Gamma = \frac{1}{4}(\sigma_1^\infty + \sigma_2^\infty) + \mathrm{i}\frac{2G_1\omega^\infty}{1+\kappa}, \quad \Gamma' = -\frac{1}{2}(\sigma_1^\infty - \sigma_2^\infty)\mathrm{e}^{-2\mathrm{i}\varpi} \tag{44}$$

with

$$\omega^\infty = \mathrm{Im}(\partial D/\partial z) \tag{45}$$

The symbols ω^∞ and $(\sigma_1^\infty + \mathrm{i}\sigma_2^\infty)$ denote the rotation and the applied principal stresses at infinity. Substituting Eqs. (38), (42) and (43) into (37) and taking $|\zeta| \gg 1$ renders

$$\mathbf{s} = \begin{bmatrix} s_a \\ s_b \end{bmatrix} \tag{46}$$

where

$$s_a = \frac{a+b}{2}\left[\Gamma + \frac{1}{2\mu_0}\left(\frac{1}{4} - \frac{\chi_1}{\mu_{r1}^2}\right)(B_{0x}^2 + B_{0y}^2)\right] \tag{47}$$

$$s_b = \frac{a-b}{2}\left[\Gamma + \frac{1}{2\mu_0}\left(\frac{1}{4} - \frac{\chi_1}{\mu_{r1}^2}\right)(B_{0x}^2 + B_{0y}^2)\right] + \frac{a+b}{2}\left[\Gamma' - \frac{1}{2\mu_0}\left(\frac{1}{2} - \frac{\mu_{r1}+\chi_1}{\mu_{r1}^2}\right)(B_{0x}^2 - 2\mathrm{i}B_{0x}B_{0y} - B_{0y}^2)\right] \tag{48}$$

By applying $\bar{\sigma} = 1/\sigma$ together with Eqs. (20), (21), (32)–(35), (37) and (39), the continuity conditions of Eq. (36) result in

$$\begin{aligned}
&\mathbf{Ar}(\sigma) + \bar{\mathbf{A}}\bar{\mathbf{s}}\sigma^{-1} - \bar{\mathbf{A}}\sum_{k=1}^{\infty}\bar{\boldsymbol{\omega}}_k\sigma^{-k} - \mathbf{A}\sum_{k=1}^{\infty}\rho^k\boldsymbol{\omega}_k\sigma^{-k} + \sum_{k=1}^{\infty}\bar{\mathbf{v}}_k\sigma^{-k} \\
&\quad = -\bar{\mathbf{A}}\bar{\mathbf{r}}\left(\frac{1}{\sigma}\right) - \mathbf{As}\sigma + \mathbf{A}\sum_{k=1}^{\infty}\boldsymbol{\omega}_k\sigma^k + \bar{\mathbf{A}}\sum_{k=1}^{\infty}\rho^k\bar{\boldsymbol{\omega}}_k\sigma^k - \sum_{k=1}^{\infty}\mathbf{v}_k\sigma^k
\end{aligned} \tag{49}$$

$$\begin{aligned}
&\mathbf{Lr}(\sigma) + \bar{\mathbf{L}}\bar{\mathbf{s}}\sigma^{-1} - \bar{\mathbf{L}}^*\sum_{k=1}^{\infty}\bar{\boldsymbol{\omega}}_k\sigma^{-k} - \mathbf{L}^*\sum_{k=1}^{\infty}\rho^k\boldsymbol{\omega}_k\sigma^{-k} + \sum_{k=1}^{\infty}\bar{\mathbf{w}}_k\sigma^{-k} \\
&\quad = -\bar{\mathbf{L}}\bar{\mathbf{r}}\left(\frac{1}{\sigma}\right) - \mathbf{Ls}\sigma + \mathbf{L}^*\sum_{k=1}^{\infty}\boldsymbol{\omega}_k\sigma^k + \bar{\mathbf{L}}^*\sum_{k=1}^{\infty}\rho^k\bar{\boldsymbol{\omega}}_k\sigma^k - \sum_{k=1}^{\infty}\mathbf{w}_k\sigma^k
\end{aligned} \tag{50}$$

where

$$\mathbf{v}_k = \mu_0 \begin{Bmatrix} \mathrm{i}(v_k + v_k^*) \\ (v_k - v_k^*) \end{Bmatrix}, \quad \mathbf{w}_k = \mu_0 \begin{Bmatrix} \mathrm{i}(w_k + w_k^*) \\ (w_k - w_k^*) \end{Bmatrix} \tag{51}$$

with

$$v_k = \begin{cases} \mu_0 \left\{ \frac{\chi_1}{4} \left[2\beta\left(\rho\bar{g} - \frac{2\bar{\beta}}{a+b}\right) - (a+b)g\bar{g} \right] + \frac{(\mu_{r1}+\chi_1)\bar{g}}{8}[4\bar{\beta} - (a-b)\bar{g}] + \frac{\bar{e}_1}{2(a+b)}\left[2\chi_2 e_1 - (\mu_{r2} + \chi_2)\rho\bar{e}_1\right] \right\} & \text{for } k = 1 \\ \frac{\mu_0 \rho^{(k-1)/2}}{8k} \left\{ 2\chi_1[(a-b)\bar{g} - 2\bar{\beta}]\left(\frac{2\beta}{a+b} - \frac{g}{\rho}\right) - (\mu_{r1} + \chi_1)\left[\frac{4\bar{\beta}^2}{(a-b)} - 4\bar{\beta}\bar{g} + \bar{g}^2(a-b)\right] \right\} & \text{for } k = 3, 5, 7, \ldots \\ 0 & \text{for } k \neq 1, 3, 5, \ldots \end{cases}$$

$$v_k^* = \begin{cases} \frac{\mu_0}{8(a+b)} \left[4\chi_1\bar{\beta}g(a+b) - (\mu_{r1} + \chi_1)(a+b)^2 g^2 - 8\chi_2 e_1 \bar{e}_1 \rho + 4(\mu_{r2} + \chi_2)e_1^2 \right] & \text{for } k = 1 \\ 0 & \text{for } k \neq 1 \end{cases}$$

$$w_k = \begin{cases} \frac{\mu_0 \chi_1}{8(\lambda_1 + 2G_1)(a+b)} \left[g\bar{g}(a+b)^2 + 2\beta\bar{g}(a-b) - 4\beta\bar{\beta} \right] - \frac{\chi_2 e_1^2}{2(\lambda_2 + 2G_2)(a+b)} & \text{for } k = 1 \\ \frac{\mu_0 \chi_1}{8(\lambda_1 + 2G_1)} [\bar{g}(a-b) - 2\bar{\beta}]\left(\frac{g}{\rho} + \frac{2\beta}{a+b}\right)\rho^{(k-1)/2} & \text{for } k = 3, 5, 7, \ldots \\ 0 & \text{for } k \neq 1, 3, 5, \ldots \end{cases}$$

$$w_k^* = \begin{cases} \mu_0 \left[\frac{-\chi_1 \bar{\beta} g}{4(\lambda_1 + 2G_1)} + \frac{\chi_2 \bar{e}_1^2 \rho}{2(\lambda_2 + 2G_2)(a+b)} \right] & \text{for } k = 1 \\ 0 & \text{for } k \neq 1 \end{cases} \tag{52}$$

Similar to the previous approach, a new set of complex functions $\boldsymbol{\xi}(\zeta)$ can be introduced on the basis of analytical continuation as

$$\boldsymbol{\xi}(\zeta) = \begin{bmatrix} \mathbf{A} & -\bar{\mathbf{A}} \\ \mathbf{L} & -\bar{\mathbf{L}}^* \end{bmatrix} \begin{bmatrix} \mathbf{r}(\zeta) \\ \sum_{k=1}^{\infty} \bar{\boldsymbol{\omega}}_k \zeta^{-k} \end{bmatrix} - \begin{bmatrix} \mathbf{A} \\ \mathbf{L}^* \end{bmatrix} \sum_{k=1}^{\infty} \rho^k \boldsymbol{\omega}_k \zeta^{-k} + \begin{bmatrix} \bar{\mathbf{A}} \\ \bar{\mathbf{L}} \end{bmatrix} \bar{\mathbf{s}} \zeta^{-1} + \sum_{k=1}^{\infty} \begin{bmatrix} \bar{\mathbf{v}}_k \\ \bar{\mathbf{w}}_k \end{bmatrix} \zeta^{-k} \tag{53}$$

for $|\zeta| > 1$ and

$$\boldsymbol{\xi}(\zeta) = \begin{bmatrix} \mathbf{A} & -\bar{\mathbf{A}} \\ \mathbf{L}^* & -\bar{\mathbf{L}} \end{bmatrix} \begin{bmatrix} \sum_{k=1}^{\infty} \boldsymbol{\omega}_k \zeta^k \\ \bar{\mathbf{r}}\left(\frac{1}{\zeta}\right) \end{bmatrix} + \begin{bmatrix} \bar{\mathbf{A}} \\ \bar{\mathbf{L}}^* \end{bmatrix} \sum_{k=1}^{\infty} \rho^k \bar{\boldsymbol{\omega}}_k \zeta^k - \begin{bmatrix} \mathbf{A} \\ \mathbf{L} \end{bmatrix} \mathbf{s}\zeta - \sum_{k=1}^{\infty} \begin{bmatrix} \mathbf{v}_k \\ \mathbf{w}_k \end{bmatrix} \zeta^k \tag{54}$$

for $|\zeta| < 1$. By Liouville's theorem, we have $\boldsymbol{\xi}(\zeta)$ as a constant function. However, this constant function corresponds to a rigid motion which can be neglected (i.e. $\boldsymbol{\xi}(\zeta) = 0$). Putting this result into Eqs. (53) and (54) and using the following formulation,

$$\begin{bmatrix} \mathbf{A} & -\bar{\mathbf{A}} \\ \mathbf{L} & -\bar{\mathbf{L}}^* \end{bmatrix}^{-1} = \begin{bmatrix} \mathbf{E}_a & \mathbf{E}_b \\ \mathbf{E}_c & \mathbf{E}_d \end{bmatrix} \tag{55}$$

where

$$\mathbf{E}_a = \begin{bmatrix} \mathrm{i}G_1\vartheta_a & -G_1\vartheta_a \\ -\mathrm{i}\kappa_2 G_1\vartheta_b & -\kappa_2 G_1 \vartheta_b \end{bmatrix}, \quad \mathbf{E}_b = \begin{bmatrix} 2G_1G_2\vartheta_a & 2\mathrm{i}G_1G_2\vartheta_a \\ -2G_1G_2\vartheta_b & 2\mathrm{i}G_1G_2\vartheta_b \end{bmatrix},$$
$$\mathbf{E}_c = \begin{bmatrix} \mathrm{i}G_2\vartheta_b & G_2\vartheta_b \\ -\mathrm{i}\kappa_1 G_2\vartheta_a & \kappa_1 G_2\vartheta_a \end{bmatrix}, \quad \mathbf{E}_d = \begin{bmatrix} -2G_1G_2\vartheta_b & 2\mathrm{i}G_1G_2\vartheta_b \\ 2G_1G_2\vartheta_a & 2\mathrm{i}G_1G_2\vartheta_a \end{bmatrix} \tag{56}$$

with

$$\vartheta_a = \frac{1}{2(G_1 + \kappa_1 G_2)}, \quad \vartheta_b = \frac{1}{2(G_2 + \kappa_2 G_1)} \tag{57}$$

we can obtain

$$\mathbf{r}(\zeta) = (\mathbf{E}_a\mathbf{A} + \mathbf{E}_b\mathbf{L}^*)\sum_{k=1}^{\infty}\rho^k\boldsymbol{\omega}_k\zeta^{-k} - (\mathbf{E}_a\bar{\mathbf{A}} + \mathbf{E}_b\bar{\mathbf{L}})\bar{\mathbf{s}}\zeta^{-1} - \sum_{k=1}^{\infty}(\mathbf{E}_a\bar{\mathbf{v}}_k + \mathbf{E}_b\bar{\mathbf{w}}_k)\zeta^{-k} \tag{58}$$

$$\sum_{k=1}^{\infty}\boldsymbol{\omega}_k\zeta^k = (\overline{\mathbf{E}}_c\bar{\mathbf{A}} + \overline{\mathbf{E}}_d\overline{\mathbf{L}}^*)\sum_{k=1}^{\infty}\rho^k\bar{\boldsymbol{\omega}}_k\zeta^k - (\overline{\mathbf{E}}_c\mathbf{A} + \overline{\mathbf{E}}_d\mathbf{L})\mathbf{s}\zeta - \sum_{k=0}^{\infty}(\overline{\mathbf{E}}_c\mathbf{v}_k + \overline{\mathbf{E}}_d\mathbf{w}_k)\zeta^k \tag{59}$$

Solving for Eq. (59) gives

$$\boldsymbol{\omega}_k = [\mathbf{I} - (\overline{\mathbf{E}}_c\overline{\mathbf{A}} + \overline{\mathbf{E}}_d\overline{\mathbf{L}}^*)(\mathbf{E}_c\mathbf{A} + \mathbf{E}_d\mathbf{L}^*)\rho^{2k}]^{-1}[(\overline{\mathbf{E}}_c\overline{\mathbf{A}} + \overline{\mathbf{E}}_d\overline{\mathbf{L}}^*)\rho^k\bar{\mathbf{y}}_k + \mathbf{y}_k] \tag{60}$$

where $\mathbf{I}$ is an 2×2 identity matrix and $\mathbf{y}_k$ are defined as

$$\mathbf{y}_k = -[(\overline{\mathbf{E}}_c\mathbf{A} + \overline{\mathbf{E}}_d\mathbf{L})\mathbf{s}\delta_{k1} + (\overline{\mathbf{E}}_c\mathbf{v}_k + \overline{\mathbf{E}}_d\mathbf{w}_k)] \quad \text{for } k = 1, 3, 5, \ldots \tag{61}$$

and the other $\mathbf{y}_k$'s vanish. It is noted that the Kronecker delta δ_{k1} equals zero except for $k = 1$. Using Eqs. (34), (56), (57) and (60), the coefficients $\boldsymbol{\omega}_k$ (for $k > 0$) can be expressed in an explicit form as

$$\boldsymbol{\omega}_k = \frac{2G_2}{1 - 4(\kappa_2G_1 - \kappa_1G_2)(G_1 - G_2)\vartheta_a\vartheta_b\rho^{2k}}\begin{Bmatrix}\omega_k^a\\ \omega_k^b\end{Bmatrix} \tag{62}$$

where

$$\begin{aligned}\omega_k^a &= [2(G_1 - G_2)\kappa_1\vartheta_a\vartheta_b\rho^k\bar{s}_b + \vartheta_b s_a]\delta_{k1} - \mu_0[2(G_1 - G_2)\vartheta_a\vartheta_b\rho^k(\kappa_1\bar{v}_k^* + 2\mathrm{i}G_1\bar{w}_k^*) - \vartheta_b(v_k - 2\mathrm{i}G_1w_k)],\\ \omega_k^b &= [2(\kappa_2G_1 - \kappa_1G_2)\vartheta_a\vartheta_b\rho^k\bar{s}_a + \kappa_1\vartheta_a s_b]\delta_{k1} + \mu_0[2(\kappa_2G_1 - \kappa_1G_2)\vartheta_a\vartheta_b\rho^k(\bar{v}_k + 2\mathrm{i}G_1\bar{w}_k) - \vartheta_a(\kappa_1v_k^* - 2\mathrm{i}G_1w_k^*)]\end{aligned} \tag{63}$$

Having the results of $\mathbf{r}(\zeta)$ and $\boldsymbol{\omega}_k$ and using Eqs. (37), (38) and (40), the functions $\phi_j(\zeta)$ and $\psi_j(\zeta)$ can now be solved and the whole magnetoelastic fields can be determined from Eqs. (26), (27) and (29)–(31). In order to focus on the effect of magnetic loading, the far field stresses σ_1^∞ and σ_2^∞ whose effect were well studied are assumed to be zero in the following illustrations.

For an elliptic inclusion in z-plane, it is pertinent to express the stress components in terms of the coordinates x' and y' which are tangent and normal to the boundary, respectively. The stress components are transformed from those on the coordinate system (x, y) as

$$\begin{bmatrix}t_{x'x'}\\ t_{y'y'}\\ t_{x'y'}\end{bmatrix} = \begin{bmatrix}\cos^2\delta_r & \sin^2\delta_r & 2\cos\delta_r\sin\delta_r\\ \sin^2\delta_r & \cos^2\delta_r & -2\cos\delta_r\sin\delta_r\\ -\cos\delta_r\sin\delta_r & \cos\delta_r\sin\delta_r & \cos^2\delta_r - \sin^2\delta_r\end{bmatrix}\begin{bmatrix}t_{xx}\\ t_{yy}\\ t_{xy}\end{bmatrix} \tag{64}$$

where δ_r is the angle between the x-axis and x'-axis as shown in Fig. 1. Since the solutions of the stress functions are complicated, it is almost impossible to obtain the maximum interfacial stress as an explicit function of the material properties and the geometric data. We can conclude from Eqs. (26), (27), (31), (37), (40), (58), (62) and (63) that the magnetoelastic stresses are related to the incident angle of magnetic induction, the ratios G_2/G_1 and $\mu_{\mathrm{r}2}/\mu_{\mathrm{r}1}$ of the material properties and the ellipticity denoted by b/a of the inclusion. Furthermore, the relevant material properties of the matrix and the inclusion are assumed to be $v_1 = v_2 = 0.3$ and $\mu_{\mathrm{r}1} = 1000$ in the following numerical examples. The condition $v_j = 0.3$ renders $\lambda_j/G_j = 1.8$. Figs. 2 and 3 display the variation of the interfacial magnetoelastic stresses on the incident angle of the applied magnetic induction with $\mu_{\mathrm{r}2}/\mu_{\mathrm{r}1} = G_2/G_1 = 0.5$ and different b/a ratios. All the stresses in the figures of the present study are presented in a dimensionless form. In these figures, $t_{x'x'}$, $t_{y'y'}$ and $t_{x'y'}$ denotes the tangential, normal and shear magnetoelastic stresses acting on the matrix along the interface. It is noted that the reference quantity $B_0^2/2\mu_0 = 400{,}000$ N/m^2 (58 psi) will be induced by a typical magnetic induction $B_0 = 1$ T (tesla). In order to clarify the character of the interfacial stresses, the extreme values of

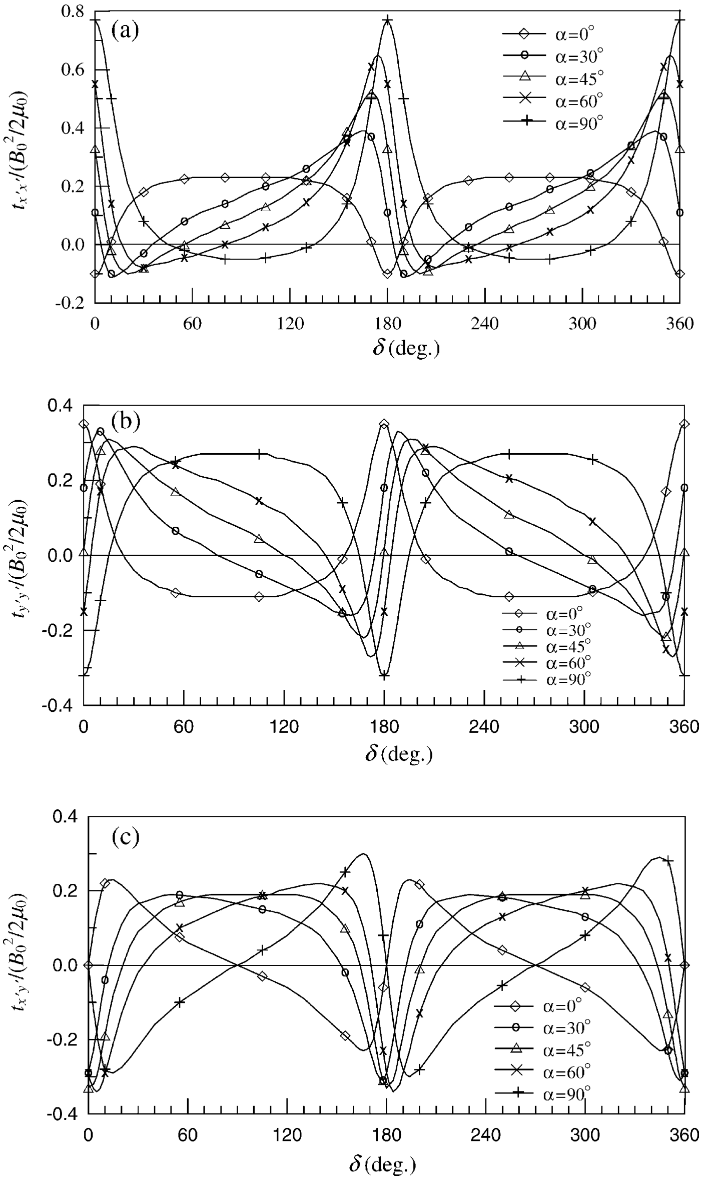

Fig. 2. Interfacial stresses on the matrix subjected to a remote uniform magnetic induction under different incident angle with $\mu_{r2}/\mu_{r1} = G_2/G_1 = 0.5$, $b/a = 0.5$: (a) $t_{x'x'}$, (b) $t_{y'y'}$, (c) $t_{x'y'}$.

the magnetoelastic stress on each curve of Figs. 2 and 3 and their corresponding angle δ are presented in Tables 1 and 2, respectively. From Figs. 2 and 3, we can find that all the distribution curves of the magnetoelastic stress have a period 180° with the angle δ. Therefore, the adding of 180° to each angle δ given in Tables 1 and 2 will lead to the same extreme value of the magnetoelastic stress. The extreme values of stress distribution tend to occur at the end of the major axis for both the tangential and the normal magnetoelastic stresses and become sharper with decreasing b/a. It is observed that the tangential stresses will increase with the incident angle α but the normal stresses decrease with increasing α. This result reveals that

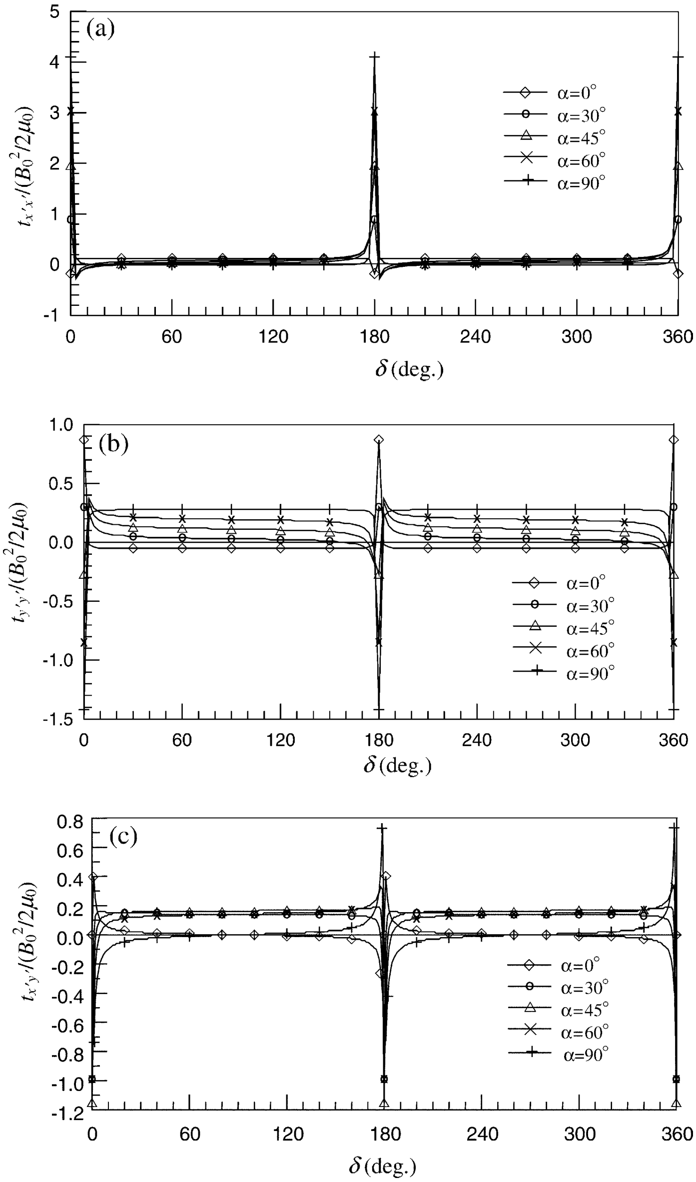

Fig. 3. Interfacial stresses on the matrix subjected to a remote uniform magnetic induction under different incident angle with $\mu_{r2}/\mu_{r1} = G_2/G_1 = 0.5$, $b/a = 0.1$: (a) $t_{x'x'}$, (b) $t_{y'y'}$, (c) $t_{x'y'}$.

the component B_{0y} of magnetic induction is the source of stress concentration and will cause singularity of the magnetoelastic stress when the inclusion approaches to a line inclusion. In Fig. 3(c), the extreme values (maximum or minimum) of the shear magnetoelastic stress for $\alpha = 0°$ and $90°$ appear in the same angle δ. For a point E located on the positive real axis, the dependence of the interfacial stress on b/a under different G_2/G_1 is shown in Fig. 4. The value of μ_{r2}/μ_{r1} is taken as 0.5 and α equals 45° in this figure. It is remarked that the magnetoelastic stresses will increase with increasing b/a and G_2/G_1. Notice that the total stresses rather than the magnetoelastic stresses are continuous across the interface between the inclusion and the

Table 1
The extreme values and circumferential angle of the magnetoelastic stresses ($b/a = 0.5$)

Extreme value	$t_{x'x'}/(B_0^2/2\mu_0)$		$t_{y'y'}/(B_0^2/2\mu_0)$		$t_{x'y'}/(B_0^2/2\mu_0)$	
	Max (δ)	Min (δ)	Max (δ)	Min (δ)	Max (δ)	Min (δ)
$\alpha = 0°$	0.23 (90°)	−0.10 (0°)	0.35 (0°)	−0.11 (90°)	0.23 (14°)	−0.23 (166°)
$\alpha = 30°$	0.39 (165°)	−0.11 (13°)	0.33 (9°)	−0.16 (160°)	0.19 (50°)	−0.31 (177°)
$\alpha = 45°$	0.52 (170°)	−0.10 (20°)	0.31 (15°)	−0.22 (168°)	0.19 (100°)	−0.31 (0°)
$\alpha = 60°$	0.65 (174°)	−0.08 (30°)	0.29 (28°)	−0.22 (172°)	0.22 (140°)	−0.34 (5°)
$\alpha = 90°$	0.77 (0°)	−0.08 (90°)	0.27 (90°)	−0.32 (0°)	0.30 (166°)	−0.30 (14°)

Table 2
The extreme values and circumferential angle of the magnetoelastic stresses ($b/a = 0.1$)

Extreme value	$t_{x'x'}/(B_0^2/2\mu_0)$		$t_{y'y'}/(B_0^2/2\mu_0)$		$t_{x'y'}/(B_0^2/2\mu_0)$	
	Max (δ)	Min (δ)	Max (δ)	Min (δ)	Max (δ)	Min (δ)
$\alpha = 0°$	0.12 (90°)	−0.18 (0°)	0.87 (0°)	−0.05 (90°)	0.40 (1°)	−0.40 (179°)
$\alpha = 30°$	0.89 (0°)	−0.23 (3°)	0.30 (0°)	−0.17 (177°)	0.16 (6°)	−0.99 (0°)
$\alpha = 45°$	1.96 (0°)	−0.28 (3°)	0.34 (3°)	−0.27 (0°)	0.19 (175°)	−1.15 (0°)
$\alpha = 60°$	3.03 (0°)	−0.22 (3°)	0.37 (3°)	−0.85 (0°)	0.33 (178°)	−0.99 (0°)
$\alpha = 90°$	4.10 (0°)	−0.01 (90°)	0.28 (90°)	−1.42 (0°)	0.73 (177°)	−0.73 (1°)

matrix. From Eqs. (19), (22), (26), (27), (31), (37), (40), (58), (62) and (63), we find that $\mu_{r1} \gg 1$ will cause insignificant Maxwell stresses. Therefore, the magnetoelastic stresses are almost continuous across the boundary for the present illustrative examples. In other words, the magnetoelastic stresses shown in Figs. 2–4 also can be regarded as the corresponding ones on the inclusion.

4. Special cases

4.1. Holes

When the inclusion is a traction free hole ($\lambda_2 = G_2 = 0$, $\mu_{r2} = 1$) within the soft ferromagnetic matrix ($\mu_{r1} \gg 1$), the mapping function in Eq. (3) will map the interior of an elliptic hole onto a circular hole. Notice that $h_2(\zeta)$ is holomorphic in S_2 which contains the origin. Therefore, the potential functions of magnetic fields induced by a uniform magnetic induction are

$$h_1(\zeta) \approx \frac{1}{\mu_0\mu_{r1}} \frac{a+b}{2} \left[(B_{0x} - \mathrm{i}B_{0y})\zeta + (B_{0x} + \mathrm{i}B_{0y})\zeta^{-1} \right] \tag{65}$$

$$h_2(\zeta) \approx \frac{2(B_{0x}b - \mathrm{i}B_{0y}a)}{\mu_0\mu_{r1}(1-\rho^2)} \left(\zeta + \rho\zeta^{-1} \right) \tag{66}$$

Thus the magnetic fields can be obtained from Eqs. (1) and (25) as

$$(H_x + \mathrm{i}H_y)_1 = \frac{1}{\mu_0\mu_{r1}} (B_x + \mathrm{i}B_y)_1 \approx \frac{1}{\mu_0\mu_{r1}(a-b)} \left[(B_{0x}a - \mathrm{i}B_{0y}b) - \frac{(B_{0x}b - \mathrm{i}B_{0y}a)\bar{z}}{\sqrt{\bar{z}^2 - (a^2-b^2)}} \right] \tag{67}$$

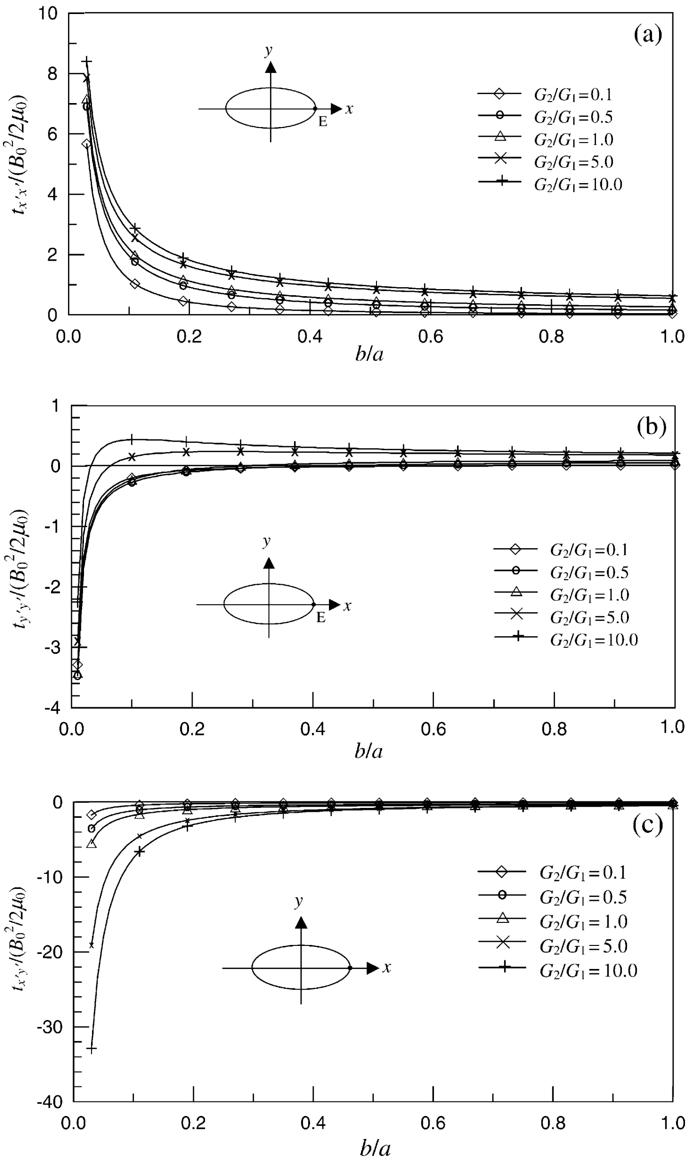

Fig. 4. Interfacial stresses at the point E ($\delta = 0°$) on the matrix subjected to a remote uniform magnetic induction of incident angle $\alpha = 45°$ with $\mu_{r2}/\mu_{r1} = 0.5$: (a) $t_{x'x'}$, (b) $t_{y'y'}$, (c) $t_{x'y'}$.

$$(H_x + iH_y)_2 = \frac{1}{\mu_0}(B_x + iB_y)_2 \approx \frac{(B_{0x}b + iB_{0y}a)}{\mu_0 \mu_{r1}} \left(\frac{1}{a} + \frac{1}{b} \right) \tag{68}$$

The comparison between Eqs. (67) and (68) indicates that the magnetic induction $(B_x + iB_y)_2$ in S_2 is much smaller than $(B_x + iB_y)_1$ in S_1. Such results guarantee the assumption that the boundary of the hole (or crack) within a soft ferromagnetic medium can be viewed as an insulated surface for magnetic fields and hence the magnetic fields inside the hole is negligible (Lin and Yeh, 2002; Lin and Lin, 2002a).

Since the inclusion is now composed of air, all the mechanical potential functions in S_2 vanish, i.e. $\phi_2(\zeta) = \psi_2(\zeta) = 0$. Referring to the previous derivations, the boundary condition of $\mathbf{f} = 0$ for a traction free hole leads to

$$\mathbf{Ar}(\sigma) + \bar{\mathbf{A}}\bar{\mathbf{s}}\sigma^{-1} + \sum_{k=1}^{\infty} \bar{\mathbf{v}}_k \sigma^{-k} = -\bar{\mathbf{A}}\bar{\mathbf{r}}\left(\frac{1}{\sigma}\right) - \mathbf{As}\sigma - \sum_{k=1}^{\infty} \mathbf{v}_k \sigma^k \tag{69}$$

By applying the method of analytical continuation, Eq. (69) yields

$$\mathbf{r}(\zeta) = -\mathbf{A}^{-1}\left(\bar{\mathbf{A}}\bar{\mathbf{s}}\zeta^{-1} + \sum_{k=1}^{\infty} \bar{\mathbf{v}}_k \zeta^{-k}\right) \approx -\mathbf{A}^{-1}\bar{\mathbf{A}}\bar{\mathbf{s}}\zeta^{-1} \tag{70}$$

where the last approximation is deduced from the estimation $(v_{2n+1}/s_a) \sim (v_{2n+1}/s_b) \sim \mathrm{O}(1/\mu_{r1}) \ll 1$.

$$\phi_1(\zeta) = s_a\zeta - \bar{s}_b\zeta^{-1}, \quad \psi_1(\zeta) = s_b\zeta - \bar{s}_a\zeta^{-1} - \frac{\rho\zeta + \zeta^{-1}}{\zeta - \rho\zeta^{-1}}\left(s_a\zeta + \bar{s}_b\zeta^{-1}\right) \tag{71}$$

If one let the minor semi-axis b approach to zero, the elliptic hole becomes a crack of length $2a$. We can obtain the magnetic fields and the corresponding magnetoelastic potential functions by taking $b = 0$ in Eqs. (17) and (19). The results are

$$h_1(\zeta) \approx \frac{a}{\mu_0\mu_{r1}}\left[(B_{0x} - \mathrm{i}B_{0y})\zeta + (B_{0x} + \mathrm{i}B_{0y})\zeta^{-1}\right] \tag{72}$$

$$h_2(\zeta) \approx \frac{a}{\mu_0\mu_{r1}}(B_{0x} - \mathrm{i}B_{0y})\zeta \tag{73}$$

Then the magnetic fields in S_1 and S_2 can be expressed as

$$(H_x + \mathrm{i}H_y)_1 = \frac{1}{\mu_0\mu_{r1}}(B_x + \mathrm{i}B_y)_1 \approx \frac{1}{\mu_0\mu_{r1}}\left(B_{0x} + \frac{\mathrm{i}B_{0y}\bar{z}}{\sqrt{\bar{z}^2 - a^2}}\right) \tag{74}$$

$$(H_x + \mathrm{i}H_y)_2 = \frac{1}{\mu_0}(B_x + \mathrm{i}B_y)_2 \approx \frac{(B_{0x} + \mathrm{i}B_{0y})}{\mu_0\mu_{r1}}\left(\frac{\bar{z}}{\sqrt{\bar{z}^2 - a^2}} + 1\right) \tag{75}$$

and

$$\phi_1(\zeta) = s_a\zeta - \bar{s}_b\zeta^{-1}, \quad \psi_1(\zeta) = s_b\zeta - \bar{s}_a\zeta^{-1} - \frac{\zeta + \zeta^{-1}}{\zeta - \zeta^{-1}}(s_a\zeta + \bar{s}_b\zeta^{-1}) \tag{76}$$

The coefficients s_a and s_b can be determined from Eqs. (47) and (48) by letting $b = 0$. For a point departed from the crack tip with a small distance along the x-axis, the stress components $t_{yy} - \mathrm{i}t_{xy}$ on it can be obtained by substituting Eqs. (74) and (76) into (31) and taking $y = 0$, $|x| > a$, (i.e. $z = \bar{z} = x$). This gives

$$t_{yy} - \mathrm{i}t_{xy} = \frac{1}{2\mu_0}(B_{0y}^2 - \mathrm{i}B_{0x}B_{0y})\frac{z}{\sqrt{z^2 - a^2}} + \mathrm{O}\left(\frac{B_0^2}{\mu_0\mu_{r1}}\right) \tag{77}$$

where $B_0^2 = B_{0x}^2 + B_{0y}^2$ and $\mu_{r1} \gg 1$. Notice that those terms with singularity order higher than $1/r^{-1/2}$ are omitted here because they will decay vary rapidly with the distance away from the crack tips (Lin and Yeh, 2002). The stress intensity factors are given as

$$(k_{\mathrm{I}} - \mathrm{i}k_{\mathrm{II}}) = \lim_{z\to a} \sqrt{2(z-a)}(t_{yy} - \mathrm{i}t_{xy}) \approx \frac{\sqrt{a}}{2\mu_0}(B_{0y}^2 - \mathrm{i}B_{0x}B_{0y}) \tag{78}$$

which is identical to the results given by Lin and Yeh (2002).

4.2. Rigid inclusion

When the inclusion is a magnetically insulated and absolutely rigid body, the magnetic function in Eqs. (65) and (66) and the magnetic fields in Eqs. (67) and (68) are also valid. The boundary condition $\mathbf{u} = 0$ renders

$$\mathbf{Lr}(\sigma) + \overline{\mathbf{L}}\bar{\mathbf{s}}\sigma^{-1} + \sum_{k=1}^{\infty} \bar{\mathbf{w}}_k \sigma^{-k} = -\overline{\mathbf{L}}\bar{\mathbf{r}}\left(\frac{1}{\sigma}\right) - \mathbf{Ls}\sigma - \sum_{k=1}^{\infty} \mathbf{w}_k \sigma^k \tag{79}$$

By applying the method of analytical continuation, Eq. (79) leads to

$$\mathbf{r}(\zeta) = -\mathbf{L}^{-1}\left(\overline{\mathbf{L}}\bar{\mathbf{s}}\zeta^{-1} + \sum_{k=1}^{\infty} \bar{\mathbf{w}}_k \zeta^{-k}\right) \approx -\mathbf{L}^{-1}\overline{\mathbf{L}}\bar{\mathbf{s}}\zeta^{-1} \tag{80}$$

The last approximation is derived from the estimation similar to that given in Eq. (70).

$$\phi_1(\zeta) = s_a\zeta + \frac{\bar{s}_b}{\kappa_1}\zeta^{-1}, \quad \psi_1(\zeta) = s_b\zeta + \kappa_1\bar{s}_a\zeta^{-1} - \frac{\rho\zeta + \zeta^{-1}}{\zeta - \rho\zeta^{-1}}\left(s_a\zeta - \frac{\bar{s}_b}{\kappa_1}\zeta^{-1}\right) \tag{81}$$

Now the elliptic rigid inclusion becomes a rigid line inclusion of length $2a$ (i.e. $b = 0$), we can obtain the stresses $t_{yy} - \mathrm{i}t_{xy}$ ahead of the crack tip along x-axis by letting $y = 0$ and $|x - a| \ll a$. It follows that

$$\begin{aligned} t_{yy} - \mathrm{i}t_{xy} &= \frac{(1-\kappa_1)}{16\mu_0\kappa_1}\left\{\left[(\kappa_1+1)B_{0x}^2 + (\kappa_1-3)B_{0y}^2\right] + 4\mathrm{i}B_{0x}B_{0y}\right\}\frac{z}{\sqrt{z^2-a^2}} \\ &\quad + \frac{(\kappa_1+1)}{16\mu_0\kappa_1}[(\kappa_1-1)B_{0x}^2 + (\kappa_1+3)B_{0y}^2 - 4\mathrm{i}B_{0x}B_{0y}] + \mathrm{O}\left(\frac{B_0^2}{\mu_0\mu_{\mathrm{r}1}}\right) \end{aligned} \tag{82}$$

Thus, the stress singularity coefficients are found as

$$(S_{\mathrm{I}} - \mathrm{i}S_{\mathrm{II}}) = \lim_{z\to a} \sqrt{2(z-a)}(t_{yy} - \mathrm{i}t_{xy}) \approx \frac{\sqrt{a}(1-\kappa_1)}{16\mu_0\kappa_1}\left\{[(\kappa_1+1)B_{0x}^2 + (\kappa_1-3)B_{0y}^2] + 4\mathrm{i}B_{0x}B_{0y}\right\} \tag{83}$$

which is identical to the results given by Lin and Lin (2002b).

4.3. Air matrix

For the case that the matrix is composed of air ($\lambda_1 = G_1 = 0$, $\mu_{\mathrm{r}1} = 1$) and the inclusion is made of ferromagnetic material, the potential functions of magnetic fields take the form

$$h_1(\zeta) \approx \frac{a+b}{2\mu_0}\left[(B_{0x} - \mathrm{i}B_{0y})\zeta - (B_{0x} + \mathrm{i}B_{0y})\zeta^{-1}\right] \tag{84}$$

$$h_2(\zeta) \approx \frac{2(B_{0x}a - \mathrm{i}B_{0y}b)}{\mu_0\mu_{\mathrm{r}2}(1-\rho^2)}(\zeta + \rho\zeta^{-1}) \tag{85}$$

The corresponding magnetic fields can be written as

$$(H_x + \mathrm{i}H_y)_1 = \frac{1}{\mu_0}(B_x + \mathrm{i}B_y)_1 \approx \frac{1}{\mu_0(a-b)}\left[-(B_{0x}b - \mathrm{i}B_{0y}a) + \frac{(B_{0x}a - \mathrm{i}B_{0y}b)\bar{z}}{\sqrt{\bar{z}^2 - (a^2 - b^2)}}\right] \tag{86}$$

$$(H_x + \mathrm{i}H_y)_2 = \frac{1}{\mu_0\mu_{r2}}(B_x + \mathrm{i}B_y)_2 \approx \frac{(B_{0x}a + \mathrm{i}B_{0y}b)}{\mu_0\mu_{r2}}\left(\frac{1}{a} + \frac{1}{b}\right) \tag{87}$$

If the applied magnetic induction is directed along y-direction (i.e. $B_{0x} = 0$), the magnetic fields $(H_x + \mathrm{i}H_y)_2$ reduce to

$$(H_x + \mathrm{i}H_y)_2 \approx \mathrm{i}\frac{B_{0y}}{\mu_0\mu_{r2}}\left(1 + \frac{b}{a}\right) \tag{88}$$

which is identical to the results derived by van de Ven (1984).

All the mechanical potential functions in S_1 vanish, i.e. $\phi_1(\zeta) = \psi_1(\zeta) = 0$, for the present case of air matrix. The condition $\mathbf{f}^* = 0$ for the traction free boundary of an elliptic inclusion yields

$$-\overline{\mathbf{A}}\sum_{k=1}^{\infty}\bar{\boldsymbol{\omega}}_k\sigma^{-k} - \mathbf{A}\sum_{k=1}^{\infty}\rho^k\boldsymbol{\omega}_k\sigma^{-k} + \sum_{k=1}^{\infty}\bar{\mathbf{v}}_k\sigma^{-k} = \mathbf{A}\sum_{k=1}^{\infty}\boldsymbol{\omega}_k\sigma^k + \overline{\mathbf{A}}\sum_{k=1}^{\infty}\rho^k\bar{\boldsymbol{\omega}}_k\sigma^k - \sum_{k=1}^{\infty}\mathbf{v}_k\sigma^k \tag{89}$$

where

$$\mathbf{v}_1 \approx \frac{a+b}{4}\mu_0\begin{bmatrix}\mathrm{i}(g^2 - 2g\bar{g} + \rho\bar{g}^2) \\ -(g^2 + 2g\bar{g} - \rho\bar{g}^2)\end{bmatrix}, \qquad \mathbf{v}_k \approx \begin{bmatrix}-\mathrm{i} \\ -1\end{bmatrix}\frac{(a+b)\rho^{n-1}\mu_0 g^2}{4(2n+1)} \quad \text{for } k = 1, 3, 5, \ldots \tag{90}$$

Applying the method of analytical continuation, we have

$$\boldsymbol{\omega}_k = \frac{\mathbf{A}^{-1}}{1-\rho^{2k}}(\mathbf{v}_k - \rho\bar{\mathbf{v}}_k) \quad \text{for } k = 1, 3, 5, \ldots \qquad \text{and} \qquad \boldsymbol{\omega}_k = 0 \quad \text{for } k \neq 1, 3, 5, \ldots \tag{91}$$

and hence the stresses can be solved from Eqs. (31), (37), (38) and (40).

For the special case of circular inclusion, the region S_2 will map onto a unit circle rather than an annulus. Referring to Eq. (31) and using the feature that the potentials $\phi_2'(\zeta)$ and $\psi_2'(\zeta)$ are holomorphic in S_2 including the origin, the general solutions of function $\Psi^*(\zeta)$ can be expressed as

$$\Psi^*(\zeta) = \mathbf{D}\boldsymbol{\omega}_1\zeta^{-1} + \sum_{k=1}^{\infty}\boldsymbol{\omega}_k\zeta^k \tag{92}$$

where

$$\mathbf{D} = \begin{bmatrix}0 & 0 \\ 1 & 0\end{bmatrix} \tag{93}$$

The boundary condition $\mathbf{f}^* = 0$ renders

$$-\bar{\mathbf{A}}\sum_{k=1}^{\infty}\bar{\boldsymbol{\omega}}_k\sigma^{-k} - \mathbf{A}\mathbf{D}\boldsymbol{\omega}_1\sigma^{-1} + \sum_{k=1}^{\infty}\bar{\mathbf{v}}_k\sigma^{-k} = \mathbf{A}\sum_{k=1}^{\infty}\boldsymbol{\omega}_k\sigma^k + \bar{\mathbf{A}}\overline{\mathbf{D}}\bar{\boldsymbol{\omega}}_1\sigma - \sum_{k=1}^{\infty}\mathbf{v}_k\sigma^k \tag{94}$$

where

$$\mathbf{v}_1 \approx \frac{\mu_0 g a}{2}\begin{bmatrix} \mathrm{i}(g-2\bar{g}) \\ -(g+2\bar{g}) \end{bmatrix}, \qquad \mathbf{v}_3 \approx \frac{\mu_0 a g^2}{6}\begin{bmatrix} -\mathrm{i} \\ -1 \end{bmatrix}, \qquad \mathbf{v}_k \approx 0 \quad \text{for } k \neq 1,3 \tag{95}$$

Solving for Eq. (94), the coefficients $\boldsymbol{\omega}_k$ can be obtained as

$$\boldsymbol{\omega}_1 = \frac{\mu_0 g a}{2}\begin{bmatrix} \bar{g} \\ -g \end{bmatrix}, \qquad \boldsymbol{\omega}_3 = \mathbf{A}^{-1}\mathbf{v}_3, \qquad \boldsymbol{\omega}_k = 0 \quad \text{for } k \neq 1,3 \tag{96}$$

The magnetoelastic stresses then can be found via the use of Eqs. (37), (38), (92), (93) and (96) and the following transformation

$$t_{rr} + t_{\theta\theta} = t_{xx} + t_{yy}, \quad t_{rr} - t_{\theta\theta} + 2\mathrm{i}t_{r\theta} = (t_{xx} - t_{yy} + 2\mathrm{i}t_{xy})\mathrm{e}^{-2\mathrm{i}\theta} \tag{97}$$

This gives the stress components

$$t_{rr}^{(2)} = \frac{1}{\mu_0}[(B_{0x}^2 + B_{0y}^2) + (B_{0x}^2 - B_{0y}^2)\cos 2\theta + 2B_{0x}B_{0y}\sin 2\theta] \tag{98}$$

$$t_{\theta\theta}^{(2)} = \frac{1}{\mu_0}\left[(B_{0x}^2 + B_{0y}^2) - (B_{0x}^2 - B_{0y}^2)\left(1 - \frac{r^2}{a^2}\right)\cos 2\theta - 2B_{0x}B_{0y}\left(1 - \frac{r^2}{a^2}\right)\sin 2\theta\right] \tag{99}$$

$$t_{r\theta}^{(2)} = \frac{1}{\mu_0}\left[2B_{0x}B_{0y}\left(1 - \frac{r^2}{a^2}\right)\cos 2\theta - (B_{0x}^2 - B_{0y}^2)\left(1 - \frac{r^2}{a^2}\right)\sin 2\theta\right] \tag{100}$$

in polar coordinates r and θ.

5. Conclusions

On the basis of the complex variable theory, a general solution for the magnetoelastic problem of the elliptic inclusion within a ferromagnetic matrix is obtained. Since the elliptic inclusion problem can cover a wide variety of particular cases, the solution provided in this paper is useful and general in the application of plane magnetoelasticity. The results of some special examples, such as elliptic hole, elliptic rigid inclusion and air matrix, are also given and analytically compared with the existing solutions. Besides, the stress intensity factors for a line crack and the stress singularity coefficients for a rigid line inclusion are also expressed in terms of material and geometric data explicitly. Distributions of the magnetoelastic stresses on the interface around the circumference of the inclusion are displayed in graphic form to illustrate the effect of the relevant parameters.

Acknowledgements

The author would like to thank the financial support by National Science Council, ROC through grant no. NSC-91-2212-E-252-001.

References

England, A.H., 1971. Complex Variable Methods in Elasticity. Wiley Interscience, New York.

Eshelby, J.D., 1957. The determination of the elastic field of an ellipsoidal inclusion, and related problems. Proceedings of the Royal Society, Series A 241, 376–396.

Fomethe, A., Maugin, G.A., 1998. On the crack mechanics of hard ferromagnets. International Journal of Non-Linear Mechanics 33, 85–95.

Gong, S.X., Meguid, S.A., 1992. A general treatment of the elastic field of an elliptical inhomogeneity under antiplane shear. ASME Journal of Applied Mechanics 59, S131–S135.

Hardiman, N.J., 1954. Elliptical elastic inclusion in an infinite elastic plane. Quarterly Journal of Mechanics and Applied Mathematics 7, 226–230.

Lin, C.B., Yeh, C.S., 2002. The magnetoelastic problem of a crack in a soft ferromagnetic solid. International Journal of Solids and Structures 39, 1–17.

Lin, C.B., Lin, H.M., 2002a. The magnetoelastic problem of cracks in bonded dissimilar materials. International Journal of Solids and Structures 39, 2807–2826.

Lin, C.B., Lin, H.M., 2002b. Explicit solution for the magnetoelastic fields with a rigid inclusion. The Chinese Journal of Mechanics—Series A 18, 109–115.

Mura, T., 1988. Inclusion problems. Applied Mechanics Review 41, 15–20.

Muskhelishvili, N.I., 1953. Some basic problems of the mathematical theory of elasticity. Noordhoff, Gronongen.

Pao, Y.H., Yeh, C.S., 1973. A linear theory for soft ferromagnetic elastic solids. International Journal of Engineering Science 11, 415–436.

Sabir, M., Maugin, G.A., 1996. On the fracture of paramagnets and soft ferromagnets. International Journal of Non-Linear Mechanics 31, 425–440.

Shindo, Y., 1977. The linear magnetoelastic problem for a soft ferromagnetic elastic solid with a finite crack. ASME Journal of Applied Mechanics 44, 47–51.

Shindo, Y., Horiguchi, K., Shindo, T., 1999. Magneto-elastic analysis of a soft ferromagnetic plate with a through crack under bending. International Journal of Engineering Science 37, 687–702.

van de Ven, A.A.F., 1984. Magnetoelastic buckling of a beam of elliptic cross-section. Acta Mechanica 51, 119–138.